peaks were recorded by collection of scattering over a limited solid angle and a smooth background was subtracted from the 'sharp' peaks. Diffuse scattering in the neighborhood was not investigated.

A previous electron microscopic examination of InTl, which included image observations of a 'mottled' pre-martensitic contrast but recorded a less-extensive survey of reciprocal space than presented here, was made by Lasalmonie & Costa (1979). Their interpretation of results, in terms of static defects, is completely in accord with present conclusions.

On a lattice-dynamic model, coupling between soft modes with polarizations along $[01\bar{1}]$ and $[10\bar{1}]$ directions (having propagation vectors along [011] and [101], respectively) would lead to the observed static displacements in the (111) plane, parallel to $[11\bar{2}]$, upon freezing of these phonons. The absence of diffuse scattering along [100]* directions indicates that phonons with [110] and $[1\bar{1}0]$ lateral displacements are not coupled. From the analysis of Bowles, Barrett & Guttman (1950) it is evident that [111] is an invariant vector during this type of phase transition. This is in complete agreement with observations and the interpretative model presented here. The really surprising result may be that freezing and coupling of phonon modes is so strong more than 170 K above the critical temperature for the martensitic phase transformation.

### References


BOWLES, J. S., BARRETT, C. S. & GUTTMAN, L. (1950). *Trans. Am. Inst. Min. Eng.* **188**, 1478-1485.

BURSILL, L. A., DOWELL, W. C. T., GOODMAN, P. & TATE, N. (1978). *Acta Cryst.* A**34**, 296-308.

DOWELL, W. C. T. & WILLIAMS, D. (1976). *Ultramicroscopy*, **1**, 43-48.

GUNTON, D. J. & SAUNDERS, G. A. (1973). *Solid State Commun.* **12**, 569-572.

HONJO, G., KODERA, S. & KITAMURA, N. (1964). *J. Phys. Soc. Jpn*, **19**, 351-367.

KASHIWASE, Y., KAINUMA, Y. & KOGISO, M. (1976). *J. Phys. Soc. Jpn*, **40**, 1707-1719.

KOMATSU, K. & TERAMOTO, K. (1966). *J. Phys. Soc. Jpn*, **21**, 1151-1159.

KOYAMA, Y. & NITTONO, O. (1981). *J. Jpn Inst. Met.* **45**, 869-877.

LASALMONIE, A. & COSTA, P. (1979). *ICOMAT* 79. Proc. 3rd. Int. Conf. on Martensitic Transformations. *Am. Soc. Met.* pp. 100-103.

NAKANISHI, N. (1979). *Prog. Mater. Sci.* **24**, 143-265.

NITTONO, O. & KOYAMA, Y. (1981). *Sci. Rep. Res. Inst. Tohoku Univ. Ser. A*, **29**, Suppl. 1, 53-60.

WILKINS, S. W., LEHMANN, M. S., FINLAYSON, T. R. & SMITH, T. F. (1982). Proc. Int. Conf. on Solid State Phase Transformations, AIME, Pennsylvania, pp. 1235-1239.


*Acta Cryst.* (1984). B**40**, 560-566

# Electron-Microscopic Study of the Structure of Metastable Oxides Formed in the Initial Stage of Copper Oxidation. II. $Cu_8O$


BY R. GUAN

*Department of Applied Physics, Osaka University*, 2-1 *Yamadaoka, Suita, Osaka* 565, *Japan and Institute of Metal Research, Academia Sinica, Shenyang, People's Republic of China*

H. HASHIMOTO

*Department of Applied Physics, Osaka University*, 2-1 *Yamadaoka, Suita, Osaka* 565, *Japan*

AND K. H. KUO

*Institute of Metal Research, Academia Sinica, Shanyang, People's Republic of China*


(*Received* 5 *March* 1984; *accepted* 3 *July* 1984)


### Abstract

Small thin metastable copper oxide crystals with the chemical composition $Cu_8O$ formed on slightly oxidized thin plates and fine particles of copper have been studied by high-resolution electron microscopy. The atomic positions of Cu and O have been determined by the analysis of electron diffraction patterns and comparison of the observed structure images with theoretical ones calculated on the basis of the dynamical theory of electron diffraction and image formation theory. Crystalline $Cu_8O$ is base-centered orthorhombic and belongs to the space group $Bmm2$ with lattice parameters $a = 5{\cdot}47$, $b = 6{\cdot}02$ and $c = 9{\cdot}34$ Å. The unit-cell volume is approximately four times larger than that of $Cu_2O$. The same oxide has also been found in copper powder which has been stored at room temperature for more than 20 years.


0108-7681/84/060560-07$01.50 

## 1. Introduction

In some body-centered cubic transition metals metastable phases have been reported which contain much lower amounts of interstitial solute atoms such as C, N or O than previously known phases. For example, $Fe_8N$ has been observed by Jack (1951), $Ta_{64}C$ by Villagrana & Thomas (1965), $Nb_8O$ by Monfort, Maisseu, Allais, Deschanvres & Delavignette (1973) and $V_8O$ and $V_8N$ by Cambini (1974). Shibahara & Hashimoto (1980) observed a tungsten oxide crystal with a lower content of O than in $WO_2$, when $WO_3$ crystals were evaporated in a vacuum of $10^{-4}$ Pa. Also, suboxides were known to appear in the initial stage of oxidation of metals. Lawless, Keneth & Bentley (1981) found $V_8O$ and $V_4O$ in the first stage of oxidation when single-crystal films of vanadium were oxidized *in situ* in an electron microscope. More recently, studies of oxidation of copper have shown a number of adsorbed oxygen-ordered structures leading to the formation of $Cu_2O$ nuclei. For a summary of this work see Howie (1981, 1983). In part I of this series, Guan, Hashimoto & Yoshida (1984) found the metastable copper suboxide $Cu_4O$. In the present paper (part II) another metastable copper suboxide, $Cu_8O$, is reported.

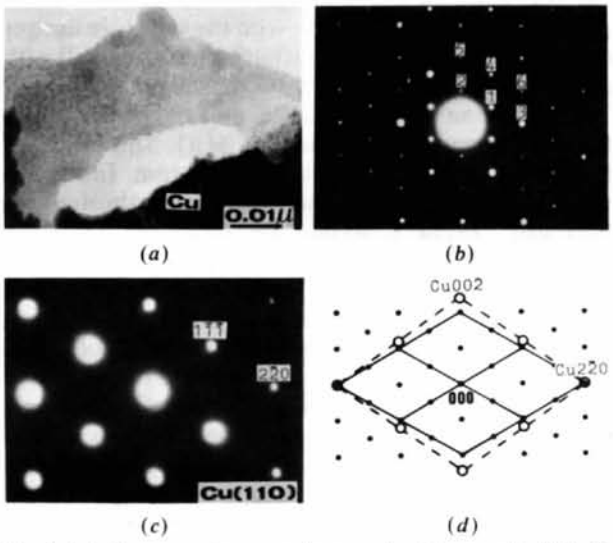


Fig. 1. (*a*) Electron-microscope image of a thin crystal of $Cu_xO$ grown at the edge of an electrolytically thinned copper film kept several days in air at room temperature. (*b*) Electron diffraction pattern of the crystal shown in (*a*). The numbering is for Table 3. (*c*) Electron diffraction pattern of the copper substrate. (*d*) Superposed diagram of the electron diffraction patterns of $Cu_xO$ (●) and copper (○).

## 2. Specimen preparation and observation

Specimens were prepared in a way similar to that described in part I (Guan, Hashimoto & Yoshida, 1984). A copper sheet 70 μm thick (purity about 99·99%), which was annealed at about 923 K in a vacuum of 2·66 Pa for 0·5 h, was electrolytically thinned to about 150 Å by the window method in nitric acid and methyl alcohol. The thin films were oxidized in air at room temperature and then observed daily for a period of two months by a JEM 100 CX electron microscope. After several days, a very thin crystal was formed at the edge of the copper film, the electron-microscope image and diffraction pattern of which are shown in Figs. 1(*a*) and 1(*b*). Fig 1(*c*) is an electron diffraction pattern of the copper substrate. Fig. 1(*d*) is a superposed diagram of Figs. 1(*b*) and 1(*c*), indicating the relation between the unknown crystal and copper.

The dimensions and thickness of the crystal shown in Fig. 1(*a*) become larger with increasing observation time. Fig. 2(*a*) shows one of the crystals which formed after the copper film had been left in air for two months. This micrograph suggests that the dimensions and thickness of this thin crystal become larger than those shown in Fig. 1(*a*) by about 100 times. It renders the same electron diffraction pattern as that shown in Fig. 1(*b*). Though nitrogen is one of the major constituents of air, it has a small sticking probability on the surface of copper, but copper combines easily with oxygen. It is therefore probable that the unknown crystal is a copper oxide. This assumption was confirmed by studying the electron energy loss spectra (EELS) of this crystal which showed clearly the edges of oxygen *K*-loss and copper *L*-loss. For simplicity, we shall refer to this phase as $Cu_xO$.

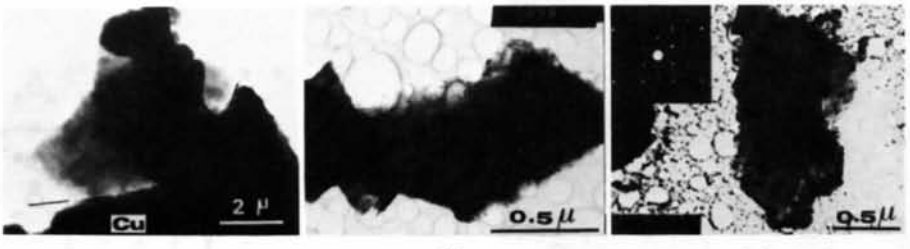


Fig. 2. Electron micrographs of (*a*) a thin crystal grown at the edge of a thin film of copper kept at room temperature in air for two months, showing the growth of the crystal (see also Fig. 1*a*) and (*b*) a $Cu_xO$ crystal found in pure copper powder stored at room temperature in contact with air for more than 20 years. (*c*) Electron micrograph and corresponding electron diffraction pattern of a $Cu_xO$ crystal formed by heating copper powder in air.

The same phase, $Cu_xO$, has also been found in commercial pure copper powder which had been stored in the Institute of Metal Research of the Academia Sinica at Shenyang for more than 20 years. Though an X-ray analysis of the powder indicated neither $Cu_2O$ nor CuO and showed no change in the lattice parameter of copper, a larger number of thin crystals with dimensions from 100 Å to 1 μm were observed under a 100 kV electron microscope. An example of these crystals is shown in Fig. 2(*b*). The corresponding electron diffraction pattern is identical to that shown in Fig. 1(*b*) and the EELS also showed peaks for oxygen and copper. A chemical analysis of the powder indicated that the oxygen content was 0·23 wt% (or 1 at.%).

Another method for obtaining this unknown $Cu_xO$ phase is to heat pure copper powder directly in air. Copper powder of about 1 μm in size was placed onto a holey-carbon film supported by a copper grid, and heated on a ceramic plate until the color of the copper grid was slightly changed. After heating, the layer of copper powder became thinner than before heating, and the $Cu_xO$ crystals appeared. An example of an electron micrograph of this material is shown in Fig. 2(*c*) together with its electron diffraction pattern. The crystals did not change in structure even after the specimen was left for three months in air.

In the present work, the first method of preparing the crystal $Cu_xO$ was mainly used. A high-resolution electron-microscope image of $Cu_xO$ is shown in Fig. 3 which was obtained with a direct magnification of about $10^6$ times. The arrangement of the bright dots is similar to the projected structure of a f.c.c. crystal in the (110) orientation with a lattice parameter about twice as large as that of copper.

### 3. Crystal structure

As described in part I (Guan, Hashimoto & Yoshida 1984), crystals of $Cu_2O$ and $Cu_4O$ grow epitaxially on the surface of copper crystals, and the O atoms generally appear as bright spots in the structure images. It is reasonable to suppose that $Cu_xO$ crystals grow with a similar crystallographic relation to the copper substrate and that the images of the O atoms appear as bright spots in the structure image of $Cu_xO$ in Fig. 3. By comparing the electron diffraction patterns of Cu and $Cu_xO$ (see Fig. 1*d*), it is clear that the basic period of $Cu_xO$ is about twice as large as that of Cu with a small expansion in the [001] direction. Based on the analyses of the structure image of $Cu_xO$ shown in Fig. 3 and its electron diffraction pattern (Fig. 1*b*), a two-dimensional structure model is presented in Fig. 4. In this model, black spots represent Cu atoms while white circles represent O atoms; the unit cell is shown as thick lines. Fig. 4 is a projection of the structure of $Cu_xO$ along the [110] direction of copper. Fig. 5 shows seven electron diffraction patterns of $Cu_xO$ in different orientations. On the basis of the analysis of all these electron diffraction patterns together with the structure images of $Cu_xO$, a base-centered orthorhombic unit cell with $a = 5{\cdot}47$, $b = 6{\cdot}02$ and $c = 9{\cdot}34$ Å was obtained.

The relationship between the unit cell of $Cu_xO$ and that of copper is shown in Fig. 6(*a*). The origin of the coordinates is placed at the Cu atom. Indices in Fig. 5 are based on this base-centered orthorhombic unit cell. Table 1 shows the ratio of two basic reciprocal-lattice vectors $\mathbf{g}_1$ and $\mathbf{g}_2$ and the angles which have been calculated from the proposed model and from the analysis of the seven electron diffraction patterns shown in Fig. 5. A good agreement of calculated and observed values suggests that the proposed model for $Cu_xO$ is correct. In the above, the origin of the unit cell was chosen at the Cu atom, but in order to show clearly the characteristics of the base-centered orthorhombic structure, the origin should preferably be chosen at the O-atom position. The unit cell of $Cu_xO$ for this choice of origin is shown in Fig. 6(*b*). The atom positions are then as shown in Table 2 with the coordinate changes of $abc(Amm2) \rightarrow bac(Bmm2)$ (Hahn, 1983).

In this model O atoms are situated in distorted tetrahedra consisting of four Cu atoms; this is similar to the structures of $Cu_4O$ and $Cu_2O$, while the

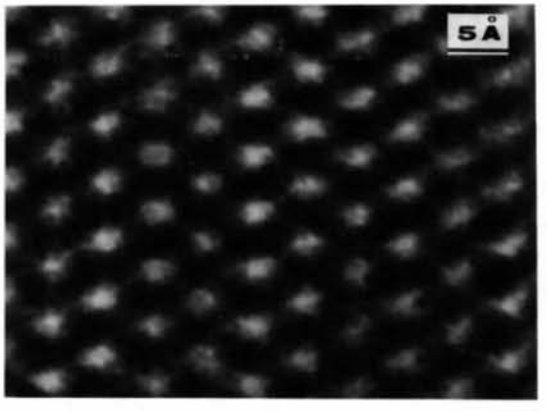


Fig. 3. A highly magnified structure image of a $Cu_xO$ crystal formed by 19 diffracted waves in Fig. 1(*d*). Direct magnification is $10^6$ times. $C_s = 0{\cdot}7$ mm, $\Delta f = 520$ Å.

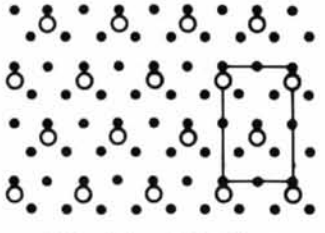

Fig. 4. Projection of Cu (●) and O (○) atoms of the structure model of $Cu_xO$ along the [110] direction of copper. The unit cell is outlined by thick lines.

Table 1. *Analysis of the electron diffraction patterns shown in Fig. 5 with reference to the* $Cu_8O$ *crystal structure*

| | | | $\mathbf{g}_2(h_2k_2l_2)/\mathbf{g}_1(h_1k_1l_1)$ | | $\varphi$ (°) | |
|---|---|---|---|---|---|---|
| *UVW* | $h_1k_1l_1$ | $h_2k_2l_2$ | Calculated | Observed | Calculated | Observed |
| 010 | $10\bar{1}$ | $\bar{1}0\bar{1}$ | 1·00 | 1·00 | 119·3 | 119·0 |
| 110 | 002 | $\bar{1}\bar{1}\bar{1}$ | 1·26 | 1·25 | 66·6 | 67·5 |
| $12\bar{1}$ | $\bar{1}0\bar{1}$ | $\bar{1}11$ | 1·27 | 1·27 | 67·4 | 68·0 |
| $22\bar{1}$ | 012 | $2\bar{1}2$ | 1·68 | 1·67 | 81·5 | 81·5 |
| $13\bar{2}$ | $1\bar{1}\bar{1}$ | $\bar{2}\bar{2}\bar{4}$ | 2·43 | 2·41 | 78·8 | 79·0 |
| $21\bar{3}$ | 111 | $3\bar{3}1$ | 2·78 | 2·90 | 81·7 | 82·0 |
| $32\bar{1}$ | $\bar{1}1\bar{1}$ | 012 | 1·00 | 1·07 | 86·3 | 86·0 |

Table 2. *Atomic coordinates of* Cu *and* O *in the* $Cu_8O$ *cell* (*space group Bmm*2)

| Element | Multiplicity | Wyckoff letter | Coordinates | | | | | | $x, y, z$ |
|---|---|---|---|---|---|---|---|---|---|
| | | | (0, | 0, | 0; | $\frac{1}{2}$, | 0, | $\frac{1}{2}$)+ | |
| Cu | 4 | *e* | $x$, | $\frac{1}{2}$, | $\bar{z}$; | $\bar{x}$, | $\frac{1}{2}$, | $\bar{z}$ | $x=\frac{1}{4}, z=\frac{3}{8}$ |
| Cu | 4 | *d* | $x$, | 0, | $\bar{z}$; | $\bar{x}$, | 0, | $\bar{z}$ | $x=\frac{1}{4}, z=\frac{3}{8}$ |
| Cu | 4 | $c_1$ | 0, | $y$, | $\bar{z}$; | 0, | $\bar{y}$, | $\bar{z}$ | $y=\frac{1}{4}, z=\frac{1}{8}$ |
| Cu | 4 | $c_2$ | 0, | $y$, | $\bar{z}$; | 0, | $\bar{y}$, | $\bar{z}$ | $y=\frac{3}{4}, z=\frac{5}{8}$ |
| O | 2 | *a* | 0, | 0, | $\bar{z}$ | | | | $z=0$ |

positions of the Cu atoms in $Cu_xO$ deviate from those in pure copper. The model gives the chemical composition of the $Cu_xO$ phase as $Cu_8O$.

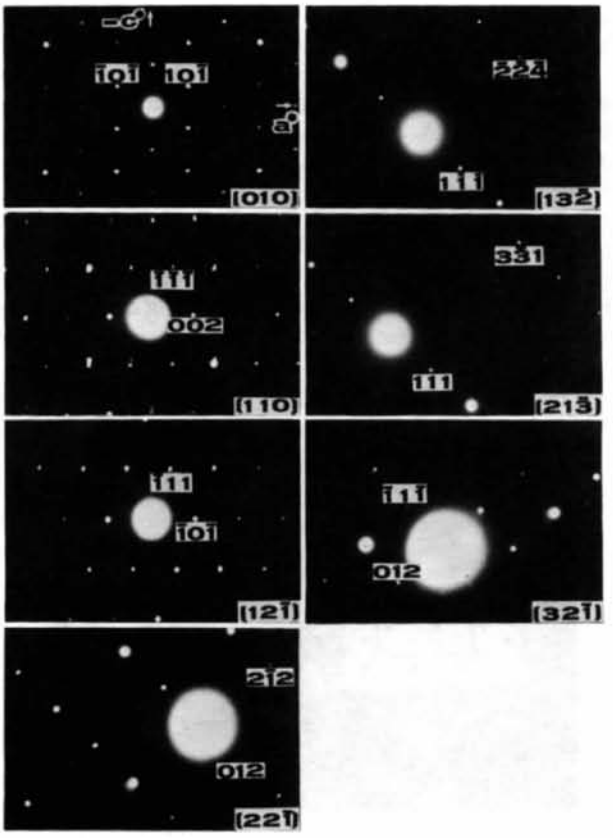


Fig. 5. Electron diffraction patterns of $Cu_8O$ for seven different orientations. Indices are based on the orthorhombic unit cell shown in Fig. 6.

## 4. Comparison of the observations with calculated data

In order to confirm the crystal structure of $Cu_8O$, the wavefield of electrons in the crystal, the intensities of the electron diffraction patterns and the intensity distribution of the electron waves at the bottom surface and the image plane resulting from the interference of the waves passing through the aperture of the objective lens have been calculated using the multislice method.

First, the amplitudes and intensities of the diffracted waves from various lattice planes of $Cu_8O$ crystals in the (010) symmetry orientation for various thicknesses were calculated. The thickness dependence of the amplitudes of several main diffracted waves is shown in Fig. 7. Though the amplitudes of the 101, 103 and 002 waves increase gradually with increasing thickness, the amplitudes of the 000, 202 and 004 waves can be seen to oscillate with a period of about 85 Å. Since the 200 amplitude behaves like the 002 and 103, it is omitted from Fig. 7 for the sake of clarity.

The calculated intensities of six electron diffraction spots from $Cu_8O$ crystals 170–180 Å thick in the (010)

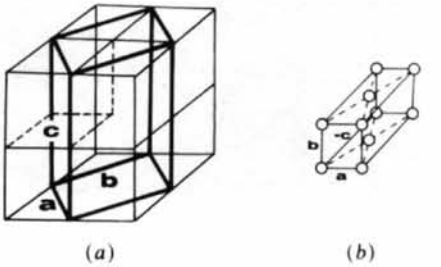


Fig. 6. (*a*) Orientation relationship between the unit cells of $Cu_8O$ (thick lines) and Cu (thin and dotted lines). (*b*) Perspective view of the base-centered orthorhombic unit cell of $Cu_8O$ crystals. Circles represent O atoms.

symmetry orientation are shown in Table 3. The calculated intensities agree well with the observed intensities of the diffraction spots shown in Fig. 1(*b*).

Figs. 8(*a*), 8(*b*) and 8(*c*) show the calculated intensities at the bottom surface of the crystals with thicknesses of 175, 120 and 85 Å, respectively. It is seen that at a thickness of 175 Å only the images of O atoms appear as large bright spots in the calculated images and that at a thickness of 120 Å only the images of Cu atoms appear as bright spots, but the images of both O and Cu atoms appear bright for a thickness of 85 Å. However, one of the pairs of bright spots in (*a*) appears at a position without any atoms. This effect seems to be due to the limited number of waves contributing to the intensity distribution.

Since the amplitudes of the diffracted waves from (202) and (004), which reflect the periodicity of the arrangement of copper, become minima at a thickness of 175 Å (see Fig. 7), the images of the Cu atoms disappear at this thickness as shown in Fig. 8(*a*). On the other hand, these waves are very strong at a thickness of 120 Å and thus the image of the Cu atoms appears as bright spots in Fig. 8(*b*). At a thickness of 85 Å, the amplitudes of the waves from (202) and (004) are nearly the same as those from (101), (103) and (002). Consequently, both Cu and O atoms appear as bright spots in Fig. 8(*c*).

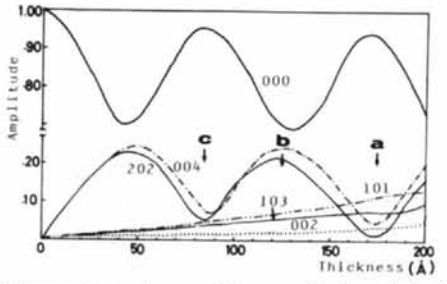


Fig. 7. Thickness dependence of the amplitudes of the diffracted waves from several atomic planes of the $Cu_8O$ structure in (010) symmetry orientation.

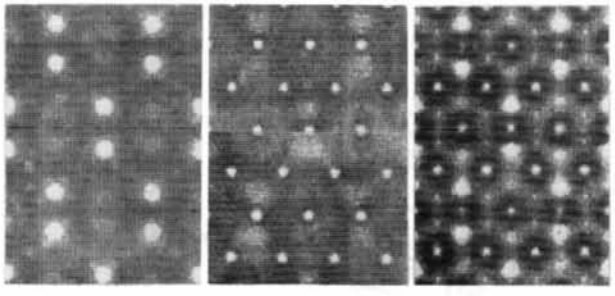

(*a*) (*b*) (*c*)

Fig. 8. Calculated intensities at the bottom surface of the crystals with thicknesses of (*a*) 175 Å, (*b*) 120 Å and (*c*) 85 Å which correspond to *a*, *b* and *c* respectively in Fig. 7. 16 384 waves are excited and the 200 waves ($g = 1{\cdot}5$ Å$^{-1}$) contributed to the intensity. See also Fig. 1(*d*).

Table 3. *Calculated intensity of electron diffraction spots from the* $Cu_8O$ *crystal in the* 010 *symmetry orientation; for the numbering of the spots, see Fig.* 1(*b*)

| No. | *hkl* | 170 Å | 180 Å |
|---|---|---|---|
| 1 | 101 | $0{\cdot}11\times10^{-1}$ | $0{\cdot}12\times10^{-1}$ |
| 2 | 002 | $0{\cdot}60\times10^{-3}$ | $0{\cdot}80\times10^{-3}$ |
| 3 | 200 | $0{\cdot}57\times10^{-2}$ | $0{\cdot}54\times10^{-2}$ |
| 4 | 103 | $0{\cdot}47\times10^{-2}$ | $0{\cdot}52\times10^{-2}$ |
| 5 | 004 | $0{\cdot}32\times10^{-2}$ | $0{\cdot}44\times10^{-2}$ |
| 6 | 202 | $0{\cdot}40\times10^{-3}$ | $0{\cdot}19\times10^{-2}$ |

The calculated intensity distribution at the image plane and the structure model of $Cu_8O$ are shown in Fig. 9 as inserts in the observed image which corresponds to Fig. 5. The parameters used in this calculation are: defocus $\Delta f = 520$ Å, spherical-aberration coefficient $C_s = 0{\cdot}7$ mm and specimen thickness $t =$ 175 Å. It is interesting to note that the contrast of the calculated images does not change when the thickness of the specimen changes within ±10 Å and the defocus within ±80 Å. A comparison of the calculated image with the observed one indicates that the agreement between them is fairly good and that the bright spots in the observed image correspond well to the O-atom positions. The disappearance of the additional spot which appears in Fig. 8(*a*) seems to be an effect due to the shape of the contrast transfer function.

Fig. 10(*a*) shows an area from the observed atomic images of $Cu_8O$, photographed with an estimated defocus of 900 Å. It shows different image contrasts at different regions indicated by letters *a*–*h*. The image of the same area taken with an estimated defocus of 500 Å is shown in Fig. 10(*b*), which shows a rather uniform contrast in the regions corresponding to the areas shown in Fig. 10(*a*). Fig. 11 shows magnified details of the areas marked in Fig. 10(*a*) together with the other areas of the same specimen image

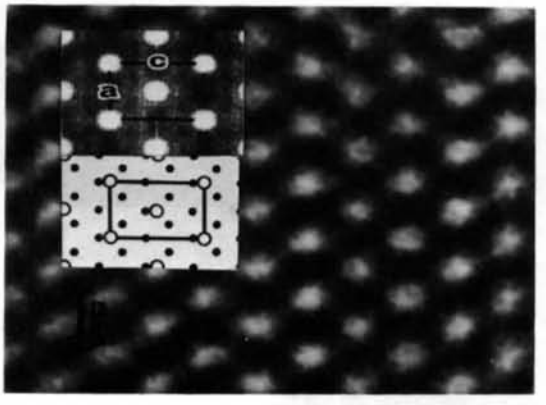


Fig. 9. Calculated image and the structure model of $Cu_8O$ with the projection of Cu and O atoms on (010) shown as insets in the observed image. Parameters used for the calculation are $\Delta f = 520$ Å, $C_s = 0{\cdot}7$ mm and thickness 170 Å.

which are not included in Fig. 10(*a*), and the calculated images obtained with different values of defocus and thickness for comparison. For such a comparison it is seen that there is a good agreement between the observed and the calculated image. The agreement suggests that the specimen has local differences in thickness. In fact, it can be seen in Fig. 1(*a*) that the thickness of the specimen is not uniform. Fig. 12 is a schematic drawing of the cross section of such a thin-film specimen on the basis of the defocus values and crystal thicknesses shown in Fig. 11. The thickness as well as the vertical position of different regions of the crystal are different. Thus the image shown in Fig. 10(*a*) represents the image of the crystal with various thicknesses taken in different focal positions at the same time. In contrast, Fig. 10(*b*) shows a uniform contrast. From the calculated images, it can be seen that, even when the defocus changes in the range 500–700 Å and the thickness in the range 160–180 Å, the image contrast does not change. Some examples of calculations are shown in Fig. 13, from which the uniform pattern shown in Fig. 10(*b*) can be understood. From the above it can be concluded that the proposed structure model of $Cu_8O$ is correct.

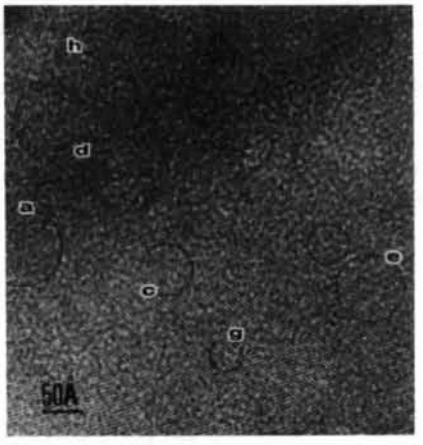


(*a*)

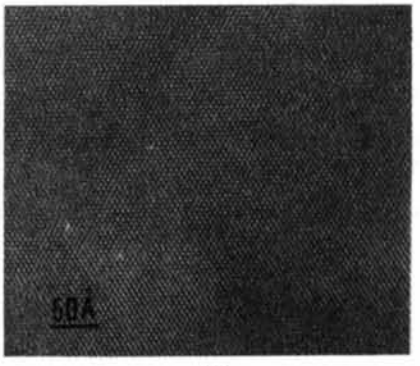


(*b*)

Fig. 10. (*a*) Magnified image of $Cu_8O$ observed at a defocus of 900 Å. (*b*) The same area as in (*a*), but at a defocus of 500 Å.

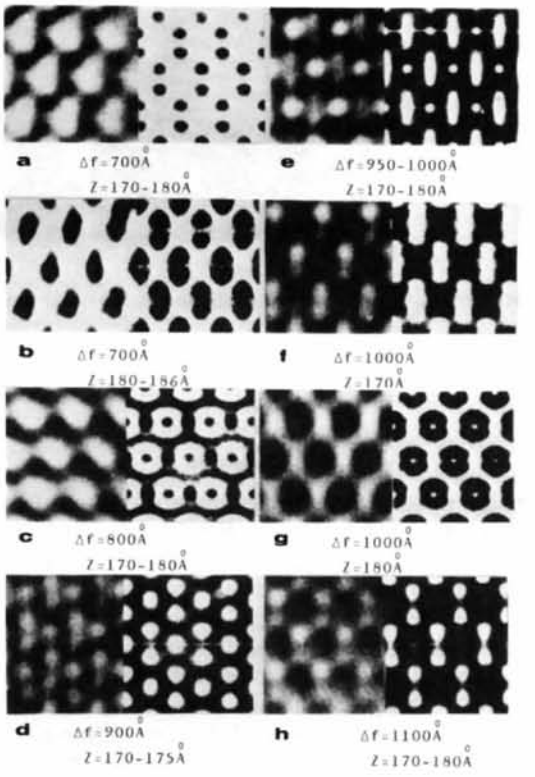


Fig. 11. Comparison of the observed and calculated images of $Cu_8O$. The magnified images on the left (*a*, *c*, *d*, *e*, *g* and *h*), taken from the encircled areas in Fig. 10(*a*), match the calculated ones on the right obtained with different values of defocus and thickness.

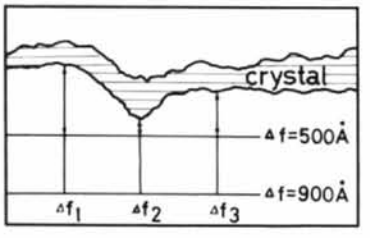


Fig. 12. Schematic cross section of a non-uniform $Cu_8O$ crystalline thin film demonstrating different defocus values in different parts of the film. $\Delta f_1$, $\Delta f_2$, $\Delta f_3$ indicate differences in defocus are obtained, when the image is taken at defocus $\Delta f = 500$ and 900 Å, in the range 700 Å–1100 Å.

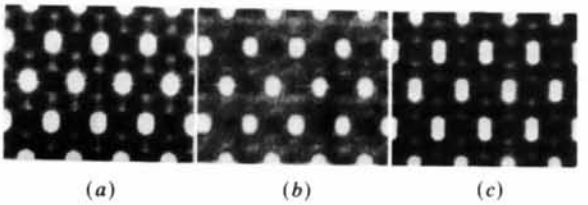

(*a*) (*b*) (*c*)

Fig. 13. Calculated images of a $Cu_8O$ crystal with thickness (*a*) 180 Å, (*b*) 174 Å, (*c*) 170 Å at a defocus of (*a*) 500 Å, (*b*) 600 Å, (*c*) 500 Å.

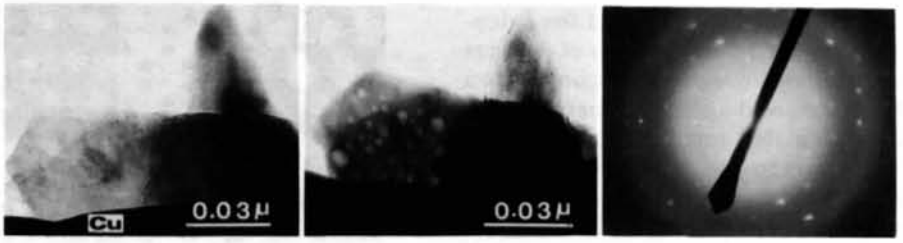


(*a*) (*b*) (*c*)

Fig. 14. (*a*) $Cu_8O$ crystal before irradiation and (*b*) after irradiation by 100 keV electrons of 1 A $cm^{-2}$ for 20 min. (*c*) Electron diffraction pattern of (*b*).

## 5. Discussion

From the observations presented above the following conclusion can be drawn. Electrolytically thinned copper films oxidized at room temperature in air for several days or pure copper powder oxidized for many years form metastable oxide crystals, $Cu_8O$, on the surface. The $Cu_8O$ crystal is very stable at room temperature in air and can be heated in high vacuum (about $10^{-4}$ Pa) without any change in structure. This is evident from the images of this crystalline film and its electron diffraction pattern. However, $Cu_8O$ cannot withstand irradiation by 100 keV electrons for longer periods of time in an electron microscope as shown in Fig. 14(*a*), (*b*) and (*c*), which shows the images made after 5 and 30 min of irradiation and the corresponding electron diffraction pattern respectively. It is seen in Fig. 14(*b*) that many thin circular regions are formed, and a diffuse electron diffraction ring appears in the corresponding electron diffraction pattern.

Most of the oxidation reactions are diffusion-controlled processes involving the inward movement of cations. The formation of $Cu_8O$ may therefore take place by a process whereby O atoms enter into the copper interstitially. Since the diffusion at room temperature is a very slow process, $Cu_8O$ forms very slowly, and it is rather difficult for a crystal nucleus to grow into a large crystal. This point is consistent with the observation that the observed $Cu_8O$ crystals have a maximum size of several microns. It was observed that the formation of $Cu_8O$ on the surface of an electrolytically thinned copper film is somewhat easier than others. This may be due to the contamination layer formed during specimen preparation. This contamination may promote the formation of $Cu_8O$ by catalytic action.

The unit cell of $Cu_8O$ contains two O and sixteen Cu atoms. The ratio of the number of O atoms to Cu atoms is one half that found in $Cu_4O$ and one quarter that found in $Cu_2O$. However, the formation mechanism of $Cu_8O$ crystals may be the same as in $Cu_4O$ and $Cu_2O$, *i.e.* $Cu_8O$ also grows epitaxially on the surface of copper crystals.

The authors would like to record their thanks to Assistant Professor H. Endoh and Dr Y. Takai for their help in carrying out the calculations and experiments and to Mr M. Tomita for his help in carrying out the image processing. Thanks are also due to Mr Y. K. Wu for helpful discussions, to Mr B. S. Zou for his help in the electron diffraction experiments and to Dr H.-U. Nissen for a critical reading of the manuscript.

### References

CAMBINI, M. (1974). *Mater. Res. Bull.* **9**, 1469–1480.

GUAN, R., HASHIMOTO, H. & YOSHIDA, T. (1984). *Acta Cryst.* B**40**, 109–114.

HAHN, T. (1983). Editor. *International Tables for Crystallography*, Vol. *A*, pp. 56–57 and 234–235. Dordrecht: Reidel.

HOWIE, A. (1981). *Inst. Phys. Conf. Ser.* No. 61, ch. 9, pp. 419–424.

HOWIE, A. (1983). *Ultramicroscopy*, **11**, 141–148.

JACK, K. H. (1951). *Proc. R. Soc. London Ser. A*, **208**, 216–224.

LAWLESS, K., KENETH, E. A. & BENTLEY, J. (1981). *Proceedings of the 39th Annual Meeting of the Electron Microscopy Society of America*, edited by G. W. BAILEY, pp. 84–85. Baton Rouge, Louisiana: Claitor's Publishing Division.

MONFORT, Y., MAISSEU, A., ALLAIS, G., DESCHANVRES, A. & DELAVIGNETTE, P. (1973). *Phys. Status Solidi A*, **15**, 129–142.

SHIBAHARA, H. & HASHIMOTO, H. (1980). *J. Appl. Cryst.* **13**, 591–596.

VILLAGRANA, R. E. & THOMAS, G. (1965). *Phys. Status Solidi*, **9**, 499–518.